Fifth International Symposium on Marine Propulsors
smp'17, Espoo, Finland, June 2017

Experience with Small Blade Area Propeller Performance

Thomas Lücke[1], Heinrich Streckwall[1]

[1]Hamburgische Schiffbau-Versuchsanstalt GmbH (HSVA), Hamburg, Germany

ABSTRACT

The need of low power consumption can lead to high efficiency propeller designs, resulting in more or less small blade area propellers in order to reduce the frictional resistance and its related efficiency loss.

Under these circumstances a model propeller will operate at comparably low Reynolds-Number (RN) due to short profile sections. This can increase the unavoidable scale effects during model tests, if they occur different at self-propulsion test (SPT) or propeller open water test (POW). The latter can affect the scaling procedures established so far, since the relation of frictional forces and frictional related pressure forces on the propeller blade may change considerably. Especially this can lead to an unusual drop of η_R, which intentionally should be free of scale effects per definition.

Further to this, these propellers often operate in conjunction with propulsion improving devices like pre-swirl stators (PSS) or behind asymmetrical aft bodies. All these examples have one pattern in common, which is the counter-swirl in the inflow of the propeller. Especially in this conjunction the interpretation of the self-propulsion factors evaluated either from experimental fluid dynamics (EFD) or computational fluid dynamics (CFD) by KT-identity is biased and leads to a further drop in η_R. If η_R deviates much from expectations or faces an unusual drop, it becomes a point of discussion.

Paint tests at low and high Reynolds-Numbers performed in the towing tank as well as in the HYKAT provide insight into the flow pattern of the boundary layer of propellers in behind- as well as open water-condition. This flow pattern shows an unexpected high amount of laminar flow, which separates usual model propellers from small blade area ratio propellers and since their corresponding propulsion behavior.

This paper summarizes results of investigations done in this respect at HSVA. By means of model tests and RANS predictions some representative problems are discussed.

Keywords

Small blade area propeller, scale effects, efficiency, laminar-separation, paint test, pre-rotating efficiency, RANS

1 INTRODUCTION

High efficiency propeller designs can lead to small blade area ratios (Ae/A0) in order to reduce the frictional resistance and its related efficiency loss. When propulsion tests with these low blade area propellers are performed, the self- propulsion factors can deviate compared to high blade area propellers. Especially the η_R values can be reduced substantially.

Small blade area propellers operate often in conjunction with propulsion improving devices like PSS or behind asymmetrical aft bodies. All these examples have one pattern in common, which is the counter swirl in the inflow of the propeller to reduce the rotational losses. Especially in this conjunction the interpretation of the self-propulsion factors evaluated either from EFD/CFD by KT-identity is biased and leads to a further drop in η_R.

In this conjunction propeller scale effects become a point of discussion. Here the crucial point is, to apply the appropriate POW characteristic, in order to separate scale-able and non-scale-able parts of the propulsion characteristic and therefore a reasonable decomposition of the behind efficiency $\eta_B = T*Vs*(1-w_{eff})/PD = \eta_0 * \eta_R$ into propeller efficiency η_0 and relative rotative efficiency η_R.

If η_R deviates much from expectations or faces an unusual drop, it becomes a point of discussion. HSVA's standard is to use one measured POW-test at high $RN_{(POW)}$ and to scale it up to to be valid for full scale $RN_{(ship)}$ and to scale it down to low $RN_{(SPT)}$ to be valid for the self-propulsion test (SPT). This is done at HSVA by means of the strip method (Streckwall 2013), which is based on local geometry particulars and friction lines, representing the frictional resistance of the propeller blade dependent on local RN=RN(r).

2 INFLUENCE OF THE PROPELLER DESIGN ONTO THE FLOW PATTERN

The wake field with its turbulence intensity and the corresponding load variations of the propeller, expressed in bound circulation Γ, in radial $\Gamma(r)$ as well as time wise dependency $\Gamma(t)$ is part of the η_R definition. The variety of surface friction lines (for flat plates), depending on the critical RN_k, show how different the flow conditions are

able to be at one single RN, see **Fig. 1**. Even slightly blunter shapes like propeller profile sections (NACA 1945) can show a different profile drag (cd_{min}) dependency on RN, showing at low-RN a different ranking between both profiles than at higher RN. The RN-dependency of the drag due to changes of the boundary layer becomes obviously dependent on the local geometry, its corresponding adverse pressure gradient and possible laminar separation.

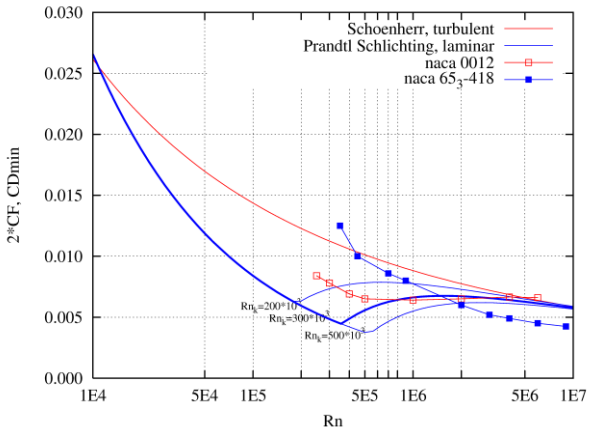

Fig. 1: Friction lines (cf) of flat plates and profile drag (cd_{min})

Propellers of high blade area ratios show sufficiently high RN during SPT- as well as POW-conditions. Small deviations in RN have no significant influence onto both performances. Applying alternative POW characteristics as the 2POW method to derive the SPT-factors lead to minor differences, indicating that the choice of them is insensible due to less RN-sensitivity. Especially at combinations of low-RN and small blade area propellers some model tests show speed dependent η_R variations instead. Hence the determination of the self-propulsion factors seems to become more sensible to small variations in RN. In these particular cases HSVA applies additionally the 2POW method, where the POW-characteristic for SPT-evaluation is directly measured by a second POW-test at an appropriate RN to meet similar flow conditions. Experience shows that the RN for this test should be about 40% higher than during the corresponding SPT. The research is still going on.

In order to investigate the sensitivity of the POW-characteristic to RN, the boundary layer has been visualized in POW- as well as SPT-conditions.

3 PROPELLER BOUNDARY LAYER VISUALISATION

Paint tests have been performed on propellers in open water and in behind condition at J-identity (J=V/(nD). The blades have been covered completely on both sides with thin layer of oil based paint. It seems to be obvious to interpret the paint test results in homogeneous flow condition, where one paint pattern is able to represent the steady flow in the blade's boundary layer. In behind condition the judgment is not as unique, since the paint pattern is only able to give one representative picture out of all different transient flow patterns during all revolutions. This has to be taken into account, when comparing the results. The results are shown exemplarily in **Figures 2-3** and **5-6** for three different propellers with different design particulars like blade area ratio per blade Ae/A0/Z, see **Table 1**. To facilitate the visual trace of the stream lines across the blades, arrows or continual lines drawn by hand are added to the original paint traces.

Table 1: Investigated Propellers

Propeller	Ae/A0/Z	$t/c_{0.7R}$	x_{rough}/c	$Rn_{0.7R}$
A	0.15	0.012	-	**3.98 10^5**
A	0.15	0.012	-	**8.76 10^5**
B	0.09	0.081	9%	1.61 10^5
C	0.15	0.041	5%	2.61 10^5

3.1 Boundary Layer of High Blade Area Propeller A

One typical high blade area propeller (**propeller A**) of a container vessel has been investigated at RN's valid for SPT ($RN_{(SPT)}$= 3.98 10^5) as well for POW ($RN_{(POW)}$=8.76 10^5), both in behind conditions in the HYKAT (Göricke 2013). The results of the paint test results are compared with the paint pattern at the corresponding POW condition at both RN.

POW vs. SPT

Figs. 2-3 show the trace of the limiting stream lines emanating from the LE and running radial outwards across the blade towards the TE, indicating mainly laminar flow regions. This flow is vulnerable to free stream conditions like turbulence in the wake field, to centrifugal forces and pressure gradients due to profile geometry (thickness to chord ratio t/c) and angle of attack (AoA). The high amount of laminar flow leads to low friction but also to more unfavorable flow around the blades and possibly to laminar separation and its loss in efficiency due to viscous form drag. In POW-condition a separation zone is clearly visible on back side near the trailing edge followed by chord wise flow line orientation, indicating turbulent flow.

Whereas at POW-condition a sudden change of flow orientation is observable, at SPT-condition this region shows only gradual changes of orientation w/o separation. The change of orientation is connected to the increase of wall shear stress due to transition into turbulent flow, which forces the flow lines to be orientated in chord wise direction.

On **face** side (lower row) no separation zone is visible at POW-condition and the change in flow orientation is similar gradual in SPT-condition (no separation on face side). The reason might be related to the much lower stream wise pressure gradient on face side in relation to back side. The face side shows similarities to the behavior of a flat plate.

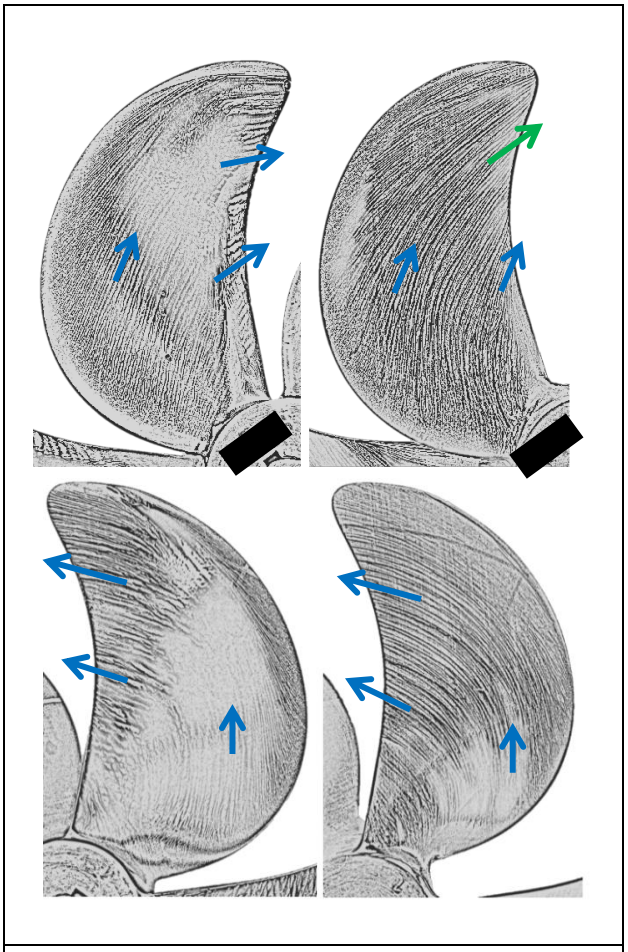

open water behind condition

Figure 2: Propeller A, RN=3.98E5,

Top row back side, bottom row face side

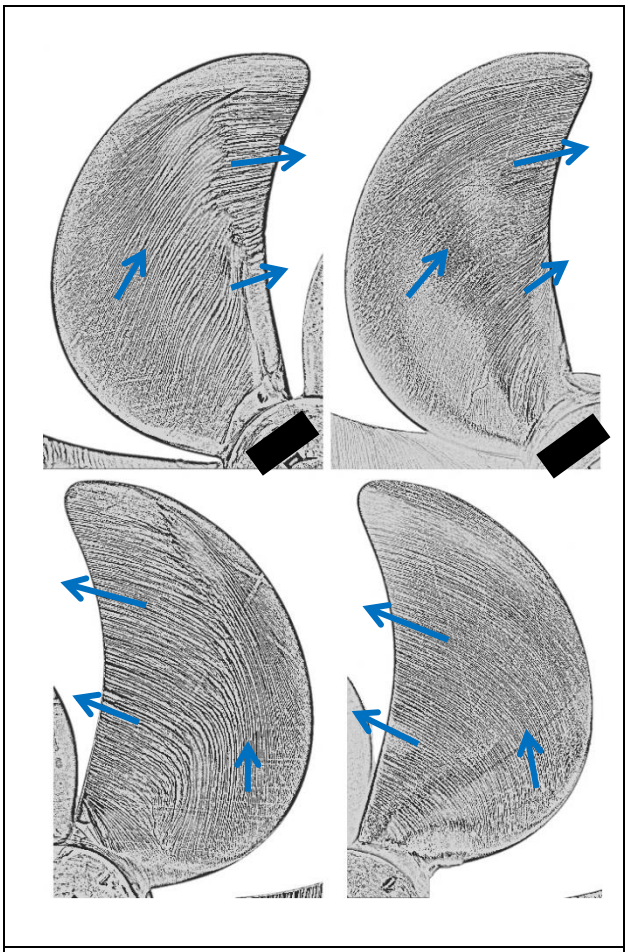

open water behind condition

Figure 3: Propeller A, RN=8.76E5,

Top row back side, bottom row face side

The flow line orientation on both sides is far from the assumption of a path along the designed radial profile sections as expected to be valid for fully turbulent flow at full scale.

Comparing the influence of inflow condition (POW vs. SPT) the left vs. right column show very similar paint patterns over the main part of the blades.

Influence of unsteadiness Γ(t)

Since the flow in open water condition is steady, the flow leads at any blade position to a more or less identical and sharp transition zone from laminar to turbulent flow. Due to the variety of AoA occurring in the transient condition many different flow patterns exist and the paint traces in the transition zone are expected to be smeared out within the whole circumference.

Influence of radial loading Γ(r)

In the time averaged sense the radial loading distribution of the propeller blade Γ(r) in the wake field corresponds to a lower tip loading and higher root loading than in homogeneous flow condition at KT-identity.

Fig. 4 shows the normalized bound circulation distribution of the propeller Γ(r) in both inflow conditions. The correspondent dependency on loading is also visible in the paint traces near the tip and the hub region. The high AoA in the tip region at POW-condition is expected to lead to the main difference between the flow orientations at SPT/POW. Due to the high lever arm this region contributes effectively to changes in torque.

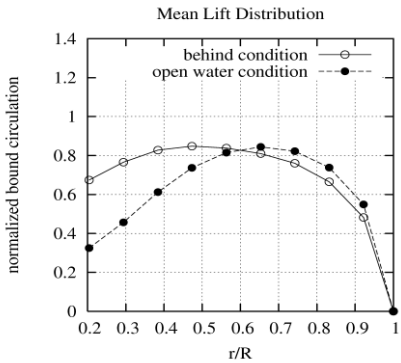

Fig. 4: Radial loading distribution Γ(r), in SPT- and POW-condition

RN-Influence

Comparing the influence of RN (**Fig. 2** vs. **Fig. 3**), the extension of the turbulent region on back side increases in radial as well as in tangential direction with increasing RN as expected. The path of the flow lines within the laminar region is not affected by the increase of RN. At low-RN the flow line orientation at the TE on back side is different (due to separation) between open water and behind condition, whereas it is similar on **face** side (indicated by green arrow). Only at high-RN the orientations near the TE are similar. On face side the transition line of the turbulent flow region extents from 0.6C to 0.5C with increasing RN.

3.2 Influence of Turbulence Stimulation by Leading Edge Roughness

The next examples deal with two propellers B (RN=1.6 10^5) and C (RN=2.6 10^5) of small and high blade area ratio respectively, see **Tab. 1,** and **Figs. 5, 6** on the next page. An artificial roughness has been applied onto the leading edge of the propellers, in order to study its influence on continuous turbulence stimulation. A special paint with a rough structured rust effect has been used to coat the leading edge of the blades over a length of 5mm (x_{rough}) which leads to relative length of 9% and 5% for propeller B and C respectively.

Above 0.7R the flow is sufficiently stipulated by roughness to become turbulent over the whole chord length. On back side the leading edge roughening at propeller B creates almost no difference in flow paths between SPT- and POW-condition. On **face** side the roughened LE influences the position of the critical radius 0.8R (for propeller B). Below these radii the flow orientation is completely unchanged.

The right column in **Fig. 5** shows the same POW-situation with smooth LE. The main difference is as expected, w/o roughness the flow is not sufficiently stipulated to be turbulent.

Considering propeller C (at higher RN) the flow paths are almost identical with and without stimulation in SPT- as well as POW-condition (besides some local phenomenon, which are assumed to be related to local irregularities). Only a very local region near the TE at POW-condition shows chord-wise flow traces which should correspond to turbulent flow. Even at higher RN the propeller C showed less sensitivity to turbulence stimulation. It seems to be a question of shape or pressure distribution rather than turbulence intensity or RN-effect (Kuiper 2010).

For both propellers the chord-wise cp-distributions (1) have been predicted by means of potential theory, which are shown for two representative radii r/R for POW-condition in **Fig. 7**.

$$cp = \frac{P - P_0}{\frac{\rho}{2}(\pi n D)^2} \qquad (1)$$

The chord length C is normalized with the shorter chord length of propeller B. The pressure distributions reveal the higher pressure level on back side of the small blade area propeller B vs. propeller C, which is necessary to attain the same thrust at the same propeller revolution rate. This corresponds to high velocity ($p \sim V^2$) on back side and corresponding thin boundary layer. Especially in the rear end ($x/c_{(PB)}$=0.6-0.7) of propeller B a much higher adverse pressure gradient on back as well as face side is visible compared to propeller C. These are the positions where the laminar separation is observed. The aforementioned turbulent stipulated flow at propeller B overcomes this unfavorable pressure gradient and avoids the separation above the critical radii. Such flow orientation is expected at higher RN e.g. for full scale.

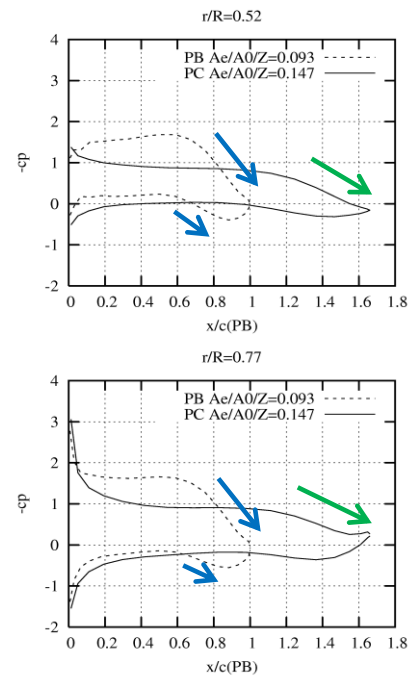

Figure 7: Chord-wise cp-distribution, Propeller B, C

The roughness at the leading edge stipulates the turbulence but it can also change the corresponding pressure distribution by diffusing or flatten it. This could reduce the chord wise pressure gradient, which is not accounted for in the present calculations. The laminar flow does not necessarily lead to high efficiency due to low frictional resistance. For a rotating propeller blade the laminar flow causes the flow paths being deviated outward due to centrifugal forces. This leads to a less favorable crosswise flow paths with possibly reduced efficiency.

This comparison shows, that in model scale even an artificial roughening at the leading edge is not always able to stimulate the flow to become turbulent.

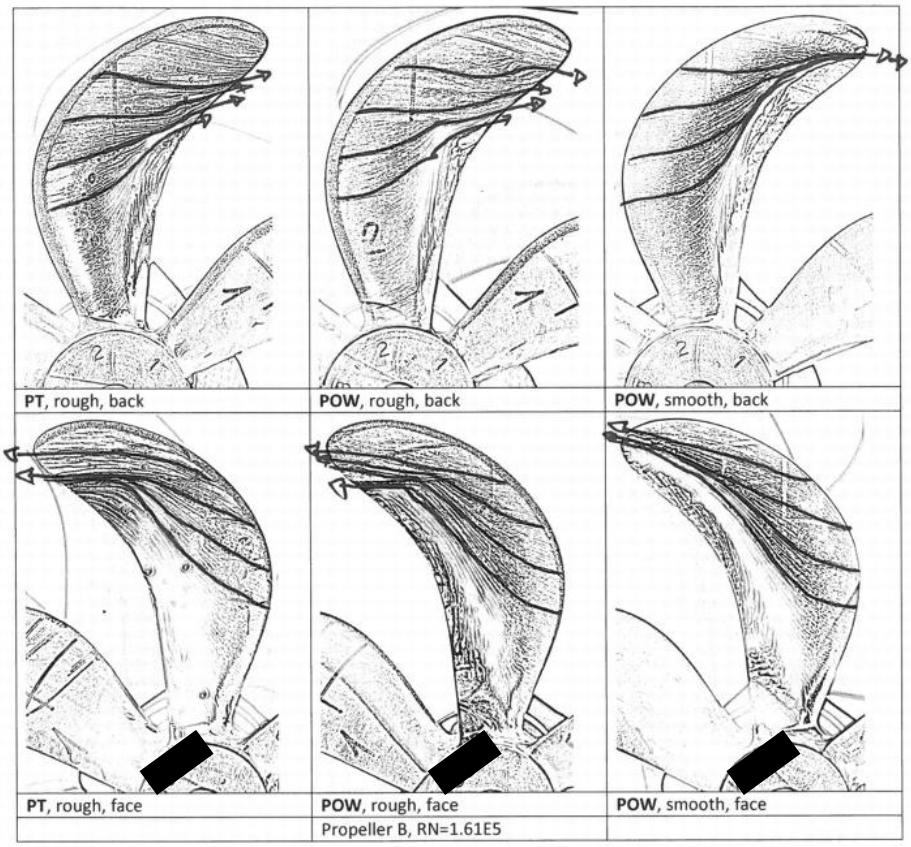

Figure 5: Propeller B, RN=1.61E5

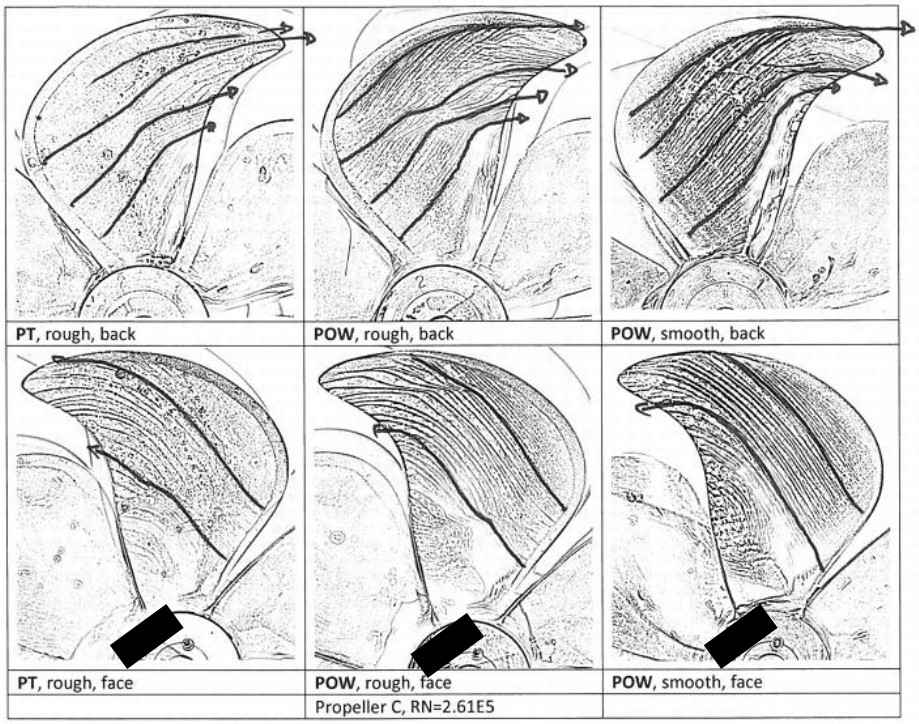

Figure 6: Propeller C, RN=2.61E5

In SPT-condition the turbulence of the wake might have a lower influence onto the propeller flow than the different propeller geometries e.g. the section shape.

Besides the low RN due to short propeller profiles, the relative higher blade thickness to chord ratio (t/c) necessary to cope with blade strength requirements plays an important role. The chord wise pressure gradient is proportional to t/c-ratio, where thick profiles are prone to separate in the rear (TE). At the same profile type, the blunt profiles have thicker leading edges and larger LE-radii than thinner profiles. These profiles behave a) more sensible against angle of attack (POW) but also b) less sensible against variations of the angle of attack within the wake field (SPT). Thick profiles with larger LE-radii accelerate the flow on back side at the LE more than thinner profiles and lead to almost chord-wise orientation of the flow lines near the LE. At low-RN the flow is initially laminar and the boundary layer is prone to separate even at moderate adverse pressure gradients.

4 POW CHARACTERISTICS AT DIFF. RN's

The link of the adverse pressure gradient, the AoA and the RN-dependency is also visible in the POW-characteristics measured at different RN's. The variety of advance coefficients J represent different angles of incidence or angles of attack. Within the relevant J of steady operation the KT and KQ curves of propellers with distinct Ae/Ao/Z show different RN-dependencies. The propeller in **Fig. 8** with Ae/A0/Z=0.15 shows more or less a similar increase in KT as well as KQ with increasing RN. On the contrary the propeller in **Fig. 9** with Ae/A0/Z=0.11 shows almost no change in KT but only in KQ. Obviously between 0.45 < J < 0.85 at certain AoA, the RN-sensitivity of KQ reaches its maximum, whereas at the border of this region (depicted by two circles) the RN-sensitivity is zero. Viscous related pressure forces act not tangential but orthogonal to the affected surface and it seems that they counteract the KT-increase due to high RN.

This is one important parameter, which separates these blades from high blade area ratio propellers.

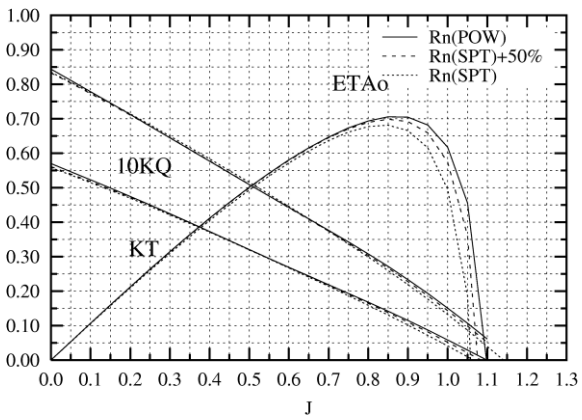

Fig. 8 : POW Characteristic, Ae/A0/Z=0.15

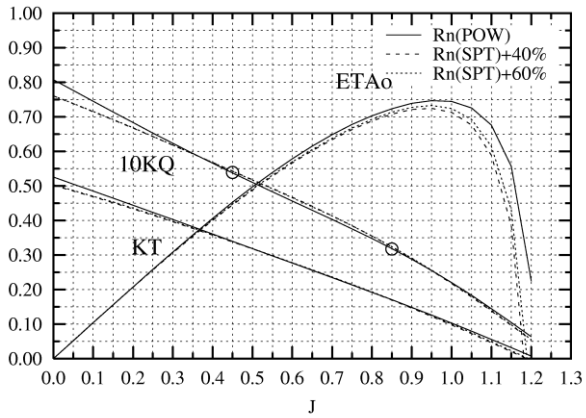

Fig. 9: POW Characteristic, Ae/A0/Z=0.11

5 INFLUENCE OF EVALUATION METHOD ON SPT-FACTORS

In conjunction with propulsion improving devices like pre swirl stators (PSS) or behind asymmetrical aft bodies the propeller works in the counter-swirl of the inflow to reduce the rotational losses. This pattern could lead to a biased interpretation of self-propulsion factors determined by KT-identity either by EFD or CFD. Especially in this conjunction the evaluation can lead to a drop in η_R, which give rise of discussions concerning either the design or the obtained results.

This inflow-swirl biases the standard interpretation of the self-propulsion factors η_0, η_R and η_H. It can have an influence onto the propeller design and its expectation, since it changes the view onto the propeller-hull interaction. A proposal from the 22nd ITTC Specialist Committee (ITTC 2008) is applied to show the possible influence onto the SPT-factors by KT- or thrust-identity, see general relations (2) and (3) for propulsion efficiency η_D.

$$\eta_D = \frac{RT*Vs}{PD} = \frac{RT*Vs}{2*\pi*N_B*Q_B} \qquad (2)$$

$$\eta_D = \frac{T*Va}{2*\pi*N_0*Q_0}*\frac{Q_0}{Q_B}*\frac{(1-t)}{(1-w)}*\frac{N_0}{N_B} = \eta_0*\eta_R*\eta_H*\eta_N \qquad (3)$$

The pre-rotating efficiency $\eta_N = n_0/n_B$ is expressed by the rate of propeller revolution n_0 in symmetrical inflow (e.g. POW) to the rate of propeller revolutions n_B in actual behind condition. For a twin screw vessel n_0 is assumed to be the arithmetic mean value between inward- outward turning direction $n_0=(n_{in}+n_{out})/2$. For vessels with PSS n_0 would be the rate of revolutions acc. to the hull w/o PSS.

Example of a Twin-Skeg

To highlight the effect of the evaluation method the results of a twin-skeg vessel are shown for model scale. At design speed the propellers have been investigated in

inward- as well as in outward-turning direction. The inward turning direction is the target sense of rotation, but the outward sense of rotation has been used in order to determine the amount of inflow-swirl in the wake field by η_N. The rudders were dismounted for this comparison in order to 1) account for the incoming swirl within the wake and 2) to separate the influence of the rudder onto the self-propulsion coefficients as well.

The propeller and its POW serve as an axial-flow measuring device, which integrates the wake field and expresses its axial velocity defect w_{eff} by means of thrust measurements. The inflow-swirl violates the applicability of the KT-identity together with the POW-characteristic.

The axial wake fraction w_{eff} in **Tab. 2**, which should only contain the axial velocity defect of the hull, shows a difference of 41% between inward- and outward rotation, if evaluated by KT-identity. Due to the corresponding shift in the advance coefficient J, the separation of $\eta_B = \eta_0 * \eta_R$ gives a biased interpretation for example of the wake adaptation of the propeller design. Especially η_H seems to be exaggerated due to a possible misinterpretation of the effective wake fraction.

The benefit of the inward turning direction of 7.6% in η_D seems to be based on a positive contribution of the η_H (+94%) by the expense of the in behind efficiency η_B (-1.5%), η_R (-0.6%) and η_0 (-1%). The benefit seems to be related to the hull by the expense of the propeller.

Table 2: Evaluation with KT- identity, inw./out., w/o rudder

design speed, model scale, w/o rudders									
	KT-identity						(rpm)	(rpm)	
out/inw	η_D	η_0	η_R	η_B	η_H	$\boldsymbol{\eta_N}$	N0	NB	weff
outw.	0.760	0.726	1.011	0.734	1.035	**1.000**	62.6	62.6	0.175
inw.	0.818	0.719	1.005	0.723	1.132	**1.000**	59.2	59.2	0.246
diff. (%)	**7.6%**	**-1.0%**	**-0.6%**	**-1.5%**	**9.4%**	**0.0%**	**-5.4%**	**-5.4%**	**40.6%**

By introducing the pre-rotating efficiency η_N in the evaluation method the bias due to the incoming swirl is separated into a **symmetric** axial wake characteristic and into the **pure homogenous swirl** of the transverse wake components. **Tab. 3** shows the comparison of the results determined by the thrust-identity method. The axial wake fraction becomes practically independent of propeller turning direction, as it should be for identical propellers behind one hull. Under this circumstance η_R increases by about 2% due to the inward sense of rotation, whereas η_0 is almost identical.

Table 3: Evaluation with thrust-identity, inw./out., w/o rudder

	thrust-identity						(rpm)	(rpm)	
out/inw	η_D	η_0	η_R	η_B	η_H	$\boldsymbol{\eta_N}$	N0	NB	weff
outw.	0.760	0.723	0.997	0.721	1.084	**0.973**	60.9	62.6	0.212
inw.	0.818	0.724	1.019	0.738	1.077	**1.029**	60.9	59.2	0.207
diff. (%)	**7.6%**	**0.1%**	**2.2%**	**2.4%**	**-0.6%**	**5.8%**	**0.0%**	**-5.4%**	**-2.4%**

Tab. 4 shows the results of the original condition with rudders and inward turning propellers. Depending on evaluation method the η_H reduces (-5.1%), η_B gains (2.3%) and η_R increases (1.4%).

Table 4: Evaluation with KT- vs. thrust-identity, inw.

with rudder, inw. turning propellers							(rpm)	(rpm)	
	η_D	η_0	η_R	η_B	η_H	$\boldsymbol{\eta_N}$	N0	NB	weff
KT-i.	0.859	0.711	1.025	0.729	1.178	**1.000**	58.5	58.5	0.275
thrust-i.	0.859	0.718	1.039	0.746	1.118	**1.029**	60.2	58.5	0.236
diff. (%)	**0.0%**	**1.0%**	**1.4%**	**2.3%**	**-5.1%**	**2.9%**	**2.9%**	**0.0%**	**-14%**

It should be noted, that the main result, the power consumption PD or η_D is practically not affected by the choice of evaluation method (KT-identity or thrust-identity). The above shows the influence of the evaluation method onto the SPT-factors, as they could be taken into account if the factors like η_R are far from expectations or a point of discussion.

Propellers operating against the sense of the inflow-swirl will face a high w_{eff} , high η_H and low η_R, if evaluated by KT-identity. The efficiency gain of PID's are therefore often interpreted as being an increase in wake fraction due to the violation of the KT-identity, rather than in η_B, but it seems to be vice versa.

Tab. 5 shows the influence of the rudder onto the propulsion characteristic (same RT, same FD). Its presence increases the wake fraction (14%) and in turn in creases η_B (1%) as well as η_R (2%).

Table 5: influence of rudder, same RT

inward turning							(rpm)	(rpm)	
	η_D	η_0	η_R	η_B	η_H	$\boldsymbol{\eta_N}$	N0	NB	weff
w/o	0.818	0.724	1.019	0.738	1.077	1.029	60.9	59.2	0.207
with	0.859	0.718	1.039	0.746	1.118	1.029	60.2	58.5	0.236
diff. (%)	**5.0%**	**-0.8%**	**2.0%**	**1.1%**	**3.8%**	**0.0%**	**-1.1%**	**-1.2%**	**14.0%**

Within the European research project INRETRO the propeller-hull interaction is investigated with particular focus on η_R. One of the examples is the single screw vessel NAWIGATOR XXI from the project partner CTO, which has been investigated experimentally and numerically as well. For the numerical analysis the HSVA RANS solver FreSCo$^+$ (Hafermann 2007) has been applied with the k-ω-SST turbulence closure model in combination with wall functions.

The results revealed that the above mentioned positive influence of the rudder onto η_R (+1.8%) is not only caused by the change of the wake field. It's also related to the local increase of thrust on the propeller cap, see **Fig. 10**. Its contribution is about 1.3% in KT due to the pressure relation on the cap, which contributes w/o disadvantages in KQ directly to η_R. This contribution amounts already 70% to the rudder influence of η_R.

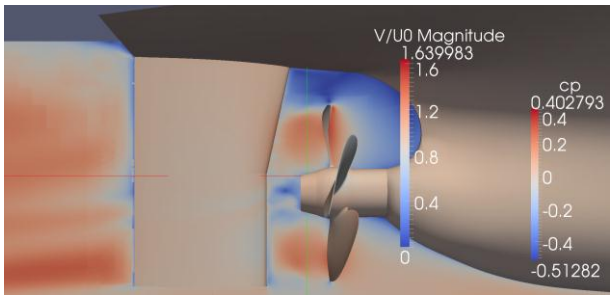

Incl. rudder: weff (+12%), Fx_{Cap}/Fx_{Prop}= +1.24%

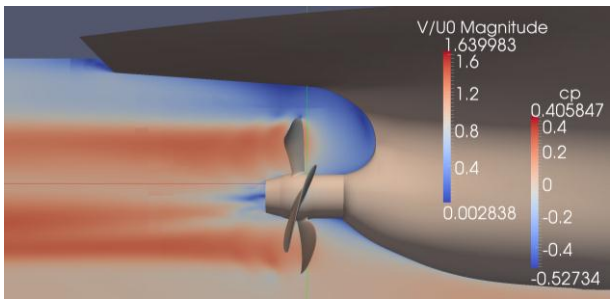

w/o rudder: Fx_{Cap}/Fx_{Prop}= -0.07%

Figure 10: Velocity distribution V/U0 on mid ship of 'Nawigator', Vs=11 kts

6 COMPARING η_R BETWEEN LOW-RN AND HIGH-RN

The relation of η_R has been investigated in the HYKAT at high-RN to check the two mentioned POW methods for consistency (HSVA standard and alternative 2POW method) especially for small blade area propellers. The high-RN is attainable in the HYKAT, since the installation of the hull with suppressed free surface allows the test to be performed above Froude-scaled speeds. **Fig. 11** shows the comparison of η_R determined by means of either HSVA standard method (strip) as well as an alternative 2POW method (at 40% higher RN) vs. results obtained in the HYKAT by means of 2POW method at high RN. On the abscissa the tank values (low-RN) and on the ordinate the HYKAT values (high-RN) are found respectively. The diagonal line represents the line of perfect correlation between the two results derived from the tank (low-RN) and the corresponding results derived in the HYKAT (high-RN). The results are presented for small blade area propellers up to an artificial threshold value of Ae/A0/Z=0.12.

Almost all results obtained at high-RN are above the correlation line showing higher η_R than at low-RN. Whereas the low-RN η_R values obtained with strip method are about 1.5% lower than the results acc. to applied 2POW method. The standard procedure seems to be conservative.

This seems to be a hint for hidden scale effects for these particular propellers, which will be investigated further.

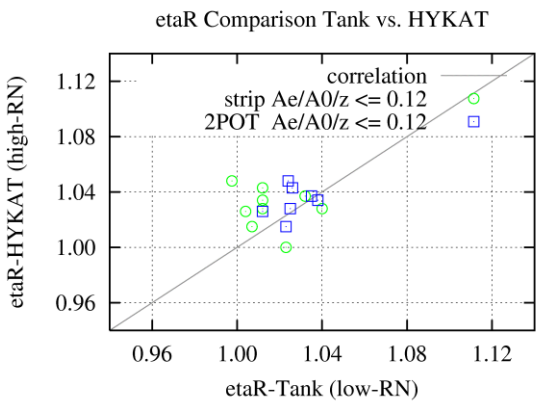

Figure 11: correlation of η_R for 2 methods vs. HYKAT 2POT, small blade area propellers

7 CONCLUSION

The influence of small blade area propellers as well as the evaluation method onto the self-propulsion factors, particularly η_R, has been discussed. By means of paint tests, the limiting stream lines of the boundary layer have been visualized. The flow pattern shows a high amount of laminar flow in POW- but as well in SPT-condition.

The main flow pattern on back and face side differ only insignificantly between the POW- and SPT-condition. The gradual change of flow line orientation at SPT-condition shows a contrast to the sharp separation zone at POW-condition. The small difference seems to be related mainly to variation of angle of attack (AoA), rather than to the turbulence intensity of the inflow.

At model scale geometry aspects and correspondent pressure gradients seem to have a higher influence on the flow pattern than RN variation or turbulence stimulation.

The rudder contributes about 1.8%-2% to η_R, whereby the main contributor is found to be the thrust on the propeller cap. Its contribution is about 1.3% in KT due to pressure relation and therefore directly to η_R. This contribution amounts already to 70% of the rudder influence of η_R.

Introducing η_N leads to an un-biased decomposition of SPT-factors if the propeller faces an inflow-swirl.

If not only the power consumption but also SPT-factors are treated as a quality index for a propeller- or ship design, the contribution of the rudder, the appropriate POW-characteristic as well as the inflow-swirl should be taken into account.

8 ACKNOWLEDGEMENT

This work is based on fruitful contributions from several colleagues of HSVA, as there are Eva Göricke, Christian Johannsen, Anke Krüger, Katrin Lassen, Julia Müller and Jens Reemts. The numerical work is part of the European INRETRO research project. The financial support by the national funding is gratefully acknowledged.

9 REFERENCES

Streckwall, H. et. al (2013). 'Development of a Strip Method Proposed to Serve as a New Standard for Propeller Performance Scaling', Ship Technology Research

Abbott, A., A.E., Doenhoff (1945). 'Summary of Airfoil data', National Advisory Committee for Aeronoutics, NACA Report No. 824

Göricke, E. L. (2013). 'Investigation of Reynolds Number Effects on the Relative Rotative Efficiency of Ship Propellers', Diploma Thesis at University Duisburg

Lücke, T. (2012). 'Off-Design – Entwicklung und Verifizierung hydrodynamisvher Berechnungs-methoden für Propulsions- und Manöverorgane im Off-Design', HSVA-Report 1671 (K03-12), Hamburgische Schiffbau-Versuchsanstalt GmbH

ITTC, (2008) The Specialist Committee on Unconventional Propulsors, "Final Report and Recommendations to the 22nd ITTC"

Streckwall, H. , Lücke, T. et. al (2016). 'Numerical Studies on Propellers in Open Water and Behind Hulls Aiming to Support the Evaluation of Propulsion Tests', NuTTs 2016

Kuiper, G.: (2010). 'Cavitation in Ship Propulsion'

Hafermann, D.: (2007), "The new RANSE Code FreSCo for Ship Application", STG Jahrbuch